Journal of Pharmaceutical Analysis 14 (2024) 100929

Contents lists available at ScienceDirect

Journal of Pharmaceutical Analysis

journal homepage: www.elsevier.com/locate/jpa

Original article

Discrimination of polysorbate 20 by high-performance liquid chromatography-charged aerosol detection and characterization for components by expanding compound database and library

Shi-Qi Wang [a, b, 1], Xun Zhao [a, 1], Li-Jun Zhang [a, b], Yue-Mei Zhao [a, c], Lei Chen [d], Jin-Lin Zhang [a], Bao-Cheng Wang [e, ****], Sheng Tang [f], Tom Yuan [g], Yaozuo Yuan [a, ***], Mei Zhang [a], Hian Kee Lee [f, h, **], Hai-Wei Shi [a, *]

[a] Jiangsu Institute for Food and Drug Control, Nanjing, 210019, China
[b] School of Pharmacy, China Pharmaceutical University, Nanjing, 211112, China
[c] School of Pharmacy, Nanjing University of Chinese Medicine, Nanjing, 210046, China
[d] Chinese Pharmacopoeia Commission, Beijing, 100061, China
[e] Nanjing Well Pharmaceutical Group Co., Ltd., Nanjing, 210018, China
[f] School of Environmental and Chemical Engineering, Jiangsu University of Science and Technology, Zhenjiang, Jiangsu, 212003, China
[g] University of Massachusetts Amherst, Amherst, 01003, USA
[h] Department of Chemistry, National University of Singapore, Singapore, 117543, Singapore

ARTICLE INFO

Article history:
Received 14 September 2023
Received in revised form
27 November 2023
Accepted 28 December 2023
Available online 30 December 2023

Keywords:
Polysorbate 20
Component
Database
Discrimination
Degradation

ABSTRACT

Analyzing polysorbate 20 (PS20) composition and the impact of each component on stability and safety is crucial due to formulation variations and individual tolerance. The similar structures and polarities of PS20 components make accurate separation, identification, and quantification challenging. In this work, a high-resolution quantitative method was developed using single-dimensional high-performance liquid chromatography (HPLC) with charged aerosol detection (CAD) to separate 18 key components with multiple esters. The separated components were characterized by ultra-high-performance liquid chromatography-quadrupole time-of-flight mass spectrometry (UHPLC-Q-TOF-MS) with an identical gradient as the HPLC-CAD analysis. The polysorbate compound database and library were expanded over 7-time compared to the commercial database. The method investigated differences in PS20 samples from various origins and grades for different dosage forms to evaluate the composition-process relationship. UHPLC-Q-TOF-MS identified 1329 to 1511 compounds in 4 batches of PS20 from different sources. The method observed the impact of 4 degradation conditions on peak components, identifying stable components and their tendencies to change. HPLC-CAD and UHPLC-Q-TOF-MS results provided insights into fingerprint differences, distinguishing quasi products.

1. Introduction

Polysorbate 20 (PS20), better known by its trade name Tween 20, is widely used as solubilizer, emulsifier, stabilizer, dispersant and/or wetting agent in biology and medicine, and food and cosmetics industries, etc., for its high biocompatibility, low toxicity and wettability [1–6]. With the in-depth research of biological agents such as vaccines, the demand for the application of polysorbate pharmaceutical excipients is constantly increasing. Typically, PS20 has high hydrophilic lipophilic equilibrium value and low critical micelle concentration, and is an efficient stabilizer in aqueous protein preparations at relatively low concentrations [7–12]. PS20 is one of the most common stabilizer used in the biopharmaceutical industry. It is a complex mixture with main components largely composed of the following three parts: sorbitan/isosorbide, polyoxyethylene (POE) with different polymerization degrees, and

* Corresponding author.
** Corresponding author. Department of Chemistry, National University of Singapore, Singapore, 117543, Singapore.
*** Corresponding author.
**** Corresponding author.
E-mail addresses: wangbch@163.com (B.-C. Wang), yyzyz7256@sina.com (Y. Yuan), chmleehk@nus.edu.sg, hiankeelee@u.nus.edu (H.K. Lee), germain0906@gmail.com (H.-W. Shi).
[1] Both authors contributed equally to this work.

https://doi.org/10.1016/j.jpha.2023.12.019

different fatty acids. The production process among different manufacturers has not been harmonized. Generally, two pathways are employed in the industrial synthesis of PS20 (Fig. S1) [13–15]. Considering the fact that water loss of sorbitol, polymerization degree of ethylene oxide and the presence of possible fatty acids in coconut oleic acid (raw material) are all difficult to control, and selection in synthetic pathways or process parameters during production are not immutable, the composition of PS20 is reported to contain more than 600 compounds [16].

Due to the uncertainty of the production process and the complexity of the components, many problems may arise during the production, storage and use of PS20 and its preparation. First of all, studies have shown that the degradation of polysorbate surfactants (especially oxidative degradation) poses a great challenge to the stability of polysorbate and its pharmaceutical products [17,18]. Degradation products of PS20 influence its overall quality. For example, PS20 will undergo auto-oxidation of the ethylene oxide chain and hydrolysis of the fatty acid chain, resulting in degradation products such as formaldehyde, acetaldehyde, formic acid, acetic acid, peroxide and free fatty acids [19–22]. Depending on usage and safety requirements, PS20 under investigation is divided into two levels based on its use in formulations: PS20 (injection) is used for injectable preparations, and PS20 (non-injection) is for non-injectable preparations. (Here, “PS20” is used to refer to PS20 generally, while “injection” or “non-injection” represents the two grades of PS20 used in different dosage forms.) Studies have shown that the more long-chain fatty acid esters are degraded in PS20, the easier it is for PS20 to nucleate and form insoluble particles; this may lead to more adverse reactions caused by biological agents intended for medical injection purposes [15]. Secondly, questionable PS20 can cause adverse reactions such as hemolysis, anaphylaxis and cytotoxicity [23–25]. Especially in the field of pharmaceuticals, the lack of understanding of the composition of some important components such as PS20 may bring unnecessary risks to drug safety regimes. There are subtle differences in PS20 from different sources. Thus, the degradation content as well as investigations based on this comparison may be a key analytical tool for quality control of PS20; however, the former have been rarely reported. In addition, the inconsistency of the production process of different manufacturers leads to the difference in the components of PS20 products from different sources, which further leads to the difference in effect [26,27]. Manufacturers of related preparations will passively continue to use PS20 products from the same supplier during the production, but be unable to actively learn the key differences between batches of this ingredient. This has caused the limitations of PS20 applications. To address this general uncertainty, a simple method to evaluate the similarity and difference between batches of different manufacturers is desirable, which is convenient for the selection of excipients in the production of preparations. With such quality assurance, it also would be very beneficial to the expansion of PS20 applications.

However, evaluation of differences amongst batches of such a complex substance is not easy. Most recent research has focused on the determination of PS20 in certain preparations using fluorescence spectrophotometry, ultraviolet-visible spectrophotometry, or high-performance liquid chromatography (HPLC) combined with charged aerosol detection (CAD) or evaporative light-scattering detection [28–34]. Few LC methods have been shown to achieve satisfactory separation of PS20. On the basis of the difficulty of separation, the lack of reference compounds makes the characterization of components even more difficult. Therefore, a detailed study has so far not been realized by LC alone [26,35]. Currently, nuclear magnetic resonance (NMR) and ultra-high performance liquid chromatography-mass spectrometry (UHPLC-MS) are often utilized for characterization of PS20 composition [36]. For example, Wang, et al. [37] qualitatively identified different polysorbate compounds by NMR, and analyzed the characteristics of the identified components by UHPLC-quadrupole time-of-flight (Q-TOF) MS [37]. The components of PS20 can also be classified into monoesters, diesters, triesters and tetraesters by matrix-assisted laser desorption ionization TOF-MS, although the different components cannot be accurately inferred [27]. Borisov, et al. [38] determined the fatty acids and assigned the components by using their characteristic fragment ions, but this method cannot ascertain the same kind of esters with different degrees of polymerization. Evers analyzed the components of PS20 by reversed-phase-UHPLC-MS, and a total of 676 compounds were obtained [16]. However, PS20 components are many more than that. Thus, for the applicability of polysorbate products whose components have high structural similarity, a simple method to differentiate PS20 from different sources based on the consideration of only a small number of key components would be desirable. This would greatly reduce the complexity of the work compared to if all the components were to be determined.

The difference in the composition of PS20 mainly comes from the manufacturing and processing. This in turn affects the quality of the product. However, current research on the complexity of components and the degree of differentiation of samples from different sources is incomplete. In addition, few studies have investigated whether degraded impurities have an impact on the composition. Moreover, most existing studies have not taken the mixed esters formed by a variety of fatty acids into consideration, and the actual components of PS20 are far more than expected [36–38]. The data used for structural characterization of PS20 or other polysorbate products are not sufficient, resulting in an incomplete component record. The comparative study of samples from different sources is even rarer, which may cause limitations in the application of PS20 and mismatches in the selection of excipients.

The current work was intended to establish a common HPLC method to achieve proper separation of complex but similar PS20 components. With this simple HPLC method, we could systematically distinguish PS20 from different sources. CAD was employed to overcome the difficulty that most PS20 components have weak ultraviolet absorption, as well as to achieve higher sensitivity, better reproducibility and simpler operation [39,40]. The HPLC-CAD method was expected to allow precise examination of PS20 composition and discern different its processes and origins, despite the complexity and diversity of formulations and sources, including variations in manufacturing processes and raw materials. It would provide a robust approach to address these variations. To further study the components of PS20 and similar polysorbate esters, as well as facilitating the deduction of existing compounds, a 7-time expansion of in-house personal compound database and library (PCDL) containing the mixed esters formed by the four most abundant fatty acids was evaluated. The chromatographic conditions developed for HPLC-CAD were then transferred to UHPLC-Q-TOF MS, for an improved understanding of PS20 components at multiple levels. Finally, spectra providing detailed information of different batches of PS20 samples were obtained (The schematic of the method is shown in Fig. 1).

2. Experimental

2.1. Reagents and chemicals

PS20 samples were obtained from six manufacturers A, B, C, D, E and F (A and C are manufacturers in China, while B, D, E and F are manufacturers from different countries.). As for the samples, A1, C1,

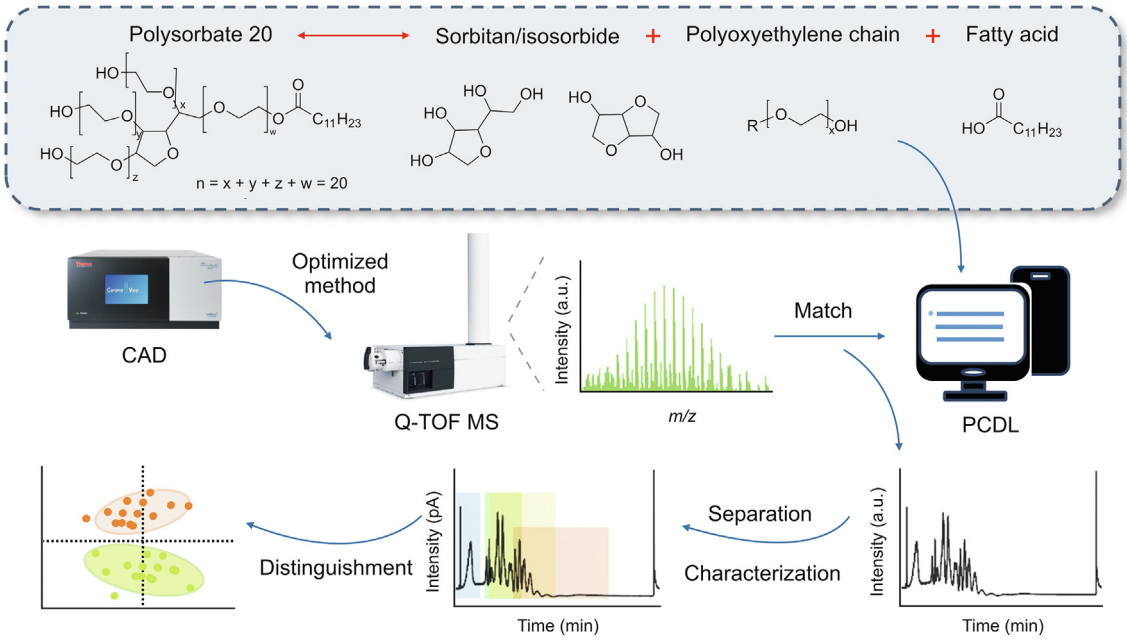

Fig. 1. Schematic of the method. PS20: polysorbate 20; CAD: charged aerosol detection; Q-TOF-MS: quadrupole time-of-flight mass spectrometry; PCDL: personal compound database and library.

C2, F1 were PS20 (non-injection); A2, B1, C3, C4, C5, D1, D2, E1 were PS20 (injection). In addition, A1, C5, D1, E1, F1 were samples outside their shelf life (expired), while A2, C1, C2, C3, C4, D2 were those still within their shelf life (unexpired). Standard reference materials were provided by Nanjing Well Pharmaceutical Corp (Nanjing, China): polyoxyethylene sorbitan (PS) (n = 30); polyoxyethylene isosorbitan (PI) (n = 24); polyoxyethylene sorbitol monolaurate (n = 42); polyoxyethylene sorbitan monolaurate (PSM-laurate) (n = 28); polyoxyethylene isosorbitan monolaurate (PIM-laurate) (n = 28); polyoxyethylene isosorbitan dilaurate (PID-di-laurate) (n = 28); polyoxyethylene isosorbitan tetralaurate (PITetra-tetra-laurate) (n = 28); polyoxyethylene sorbitol hexalaaurate (n = 42). Both HPLC- and MS-grade of acetonitrile (ACN) were obtained from Merck (Darmstadt, Germany). MS-grade formic acid was purchased from Anaqua Chemicals Supply (Boston, MA, USA). Ultra-pure water was produced using a Milli-Q-plus ultra-pure water system from Merck Millipore (Burlington, MA, USA).

2.2. Sample preparation

The PS20 sample solution was prepared at 1 mg/mL concentration in ACN. The blank solution was ACN. Sample solutions and the blank solution were analyzed by HPLC-CAD. A 0.5 mg/mL PS20 solution was diluted by ACN and filtered through a 0.22 μm membrane. The filtrate was used for UHPLC-Q-TOF-MS analysis. The specific preparation processes are given in the Supplementary data.

2.3. HPLC-CAD analysis

Analysis was performed on a Vanquish HPLC system from ThermoFisher Scientific (Waltham, MA, USA) equipped with an auto-sampler, a temperature-controlled column compartment, a binary gradient, and a CAD detector. Seven columns were preliminarily evaluated (see Supplementary data for details). The column used for the final method was a Waters Xbridge C_{18} column (4.6 mm × 250 mm, 5 μm; Milford, MA, USA). Solvent A was 0.05% formic acid in water, and solvent B was 0.05% formic acid in ACN. The separation was achieved using gradient elution: 0–15.99 min, 15%–100% B; 15.99–56 min, 100% B; 56–56.2 min, 100%–15% B; 56.2–60 min, 15% B. The column temperature was set at 50 °C. The flow rate was 1 mL/min, and the injection volume was 10 μL. The following parameters of CAD were set: nebulization temperature, 50 °C; power rate, 1.00; sampling frequency, 20 Hz; and power function value, 1.00.

2.4. UHPLC-Q-TOF-MS analysis

Analysis was performed on an Agilent 1290 series UHPLC system coupled with an Agilent 6550 Q-TOF MS equipped with an electrospray ionization (ESI) source from Agilent Technologies (Palo Alto, CA, USA). The LC method used here was the same as that given above. Half of the sample solution was split into the MS detector with a total injection volume of 10 μL. The parameters of MS were set as follows: drying gas temperature (250 °C, 12 L/min), nebulizer pressure (0.18 MPa), sheath gas temperature (350 °C, 11 L/min), capillary voltage (4.0 kV), nozzle voltage (500 V), and fragmentor voltage (160 V). MS data were collected in the m/z range of 100–3000. Mass Hunter PCDL Manager B.08.00 software and Mass Hunter Qualitative Analysis 10.0 software (Agilent Technologies) were used in the analysis.

3. Results and discussion

3.1. Method development and optimization

The method was optimized by investigating four chromatographic columns: mobile phase modifier (0.05%, 0.1% and 0.2% formic acid, sample solutions and blank solution were analyzed, respectively), gradient elution (0–3, 5, 8, 10, and 15.99 min, 15%–100% B) and run time (40, 55, 60, 120 min) (See Fig. S2 for details). For comprehensive consideration of separation, baseline stability and peak shape, Waters Xbridge C_{18} column (4.6 mm × 250 mm, 3.5 μm) and 0.05 % formic acid were chosen. The gradient of

0–15.99 min, 15%–100% B and the run time of 60 min were selected. These conditions were applied to both HPLC-CAD and UHPLC-Q-TOF-MS analysis.

3.2. Separation and confirmation of PS20 composition

PS20 components were separated with an optimized HPLC-CAD method and 18 chromatographic peaks were obtained. Theoretically PS20 contains 11 types of components: POE, PS, PI, polyoxyethylene monoesters (PM), polyoxyethylene sorbitan monoesters (PSM), polyoxyethylene isosorbitan monoesters (PIM), polyoxyethylene diesters (PD), polyoxyethylene sorbitan diesters (PSD), polyoxyethylene isosorbitan diesters (PID), polyoxyethylene sorbitan triesters (PSTri), and polyoxyethylene sorbitan tetraesters (PSTetra). A typical chromatogram is shown in Fig. 2A. At the same time, different standard reference materials (if the reference

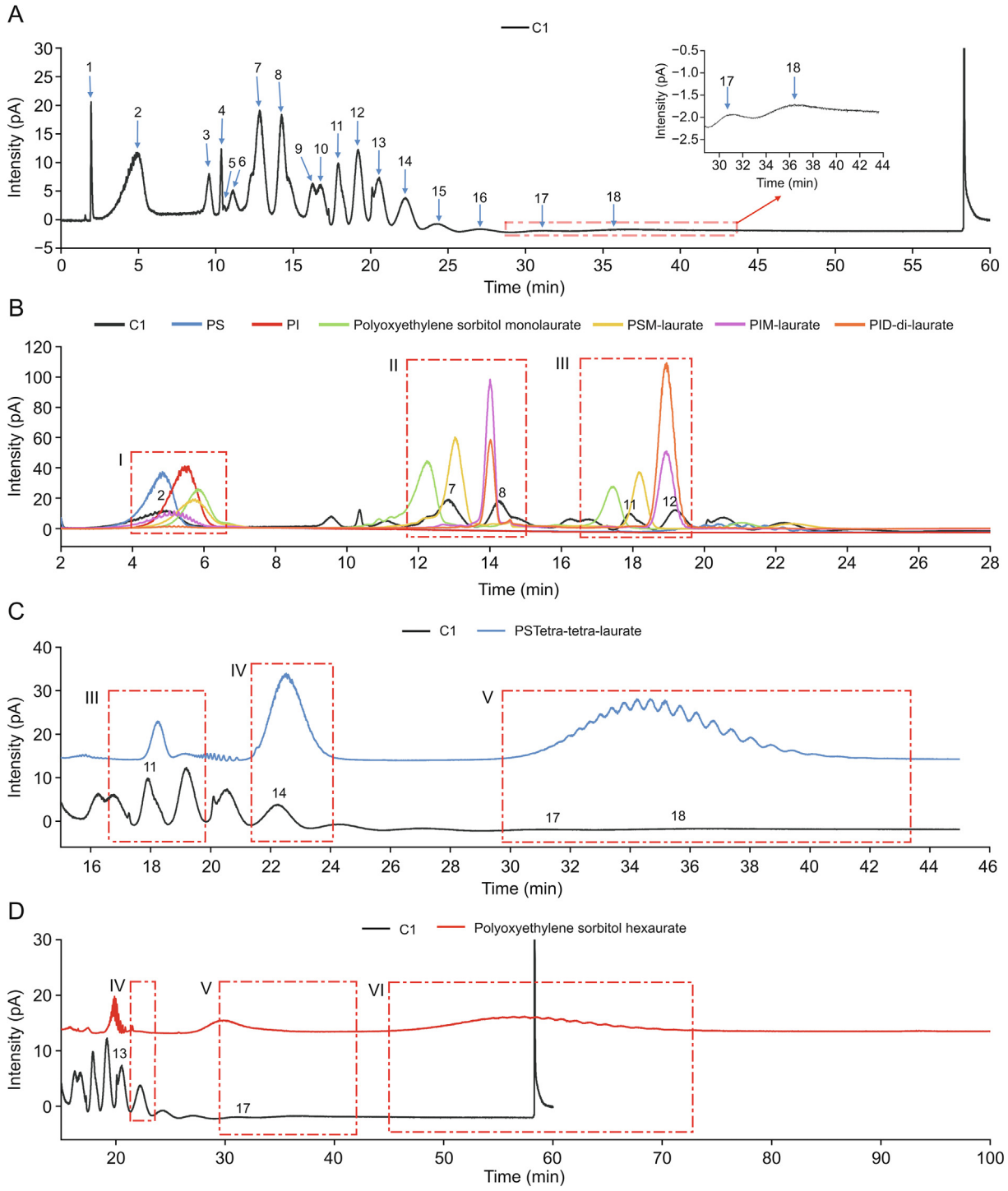

Fig. 2. Typical chromatogram of polysorbate 20 (PS20) and preliminary localization inference of its components by high-performance liquid chromatography with charged aerosol detection ((HPLC-CAD) (sample C1). (A) Sample determined by HPLC-CAD. (B) Polyoxyethylene sorbitan (PS)/polyoxyethylene isosorbitan (PI), monoesters and diesters. (C) Tetraesters. (D) Hexaesters. PSM: polyoxyethylene sorbitan monoesters; PIM: polyoxyethylene isosorbitan monoesters ; PID: polyoxyethylene isosorbitan diesters; PSTetra: polyoxyethylene sorbitan tetraesters.

material is an ester, it is laurate) were synthesized and used for accurate positioning of the peaks (Figs. 2B–2D).

However, during the peak confirmation process, it was found that the two peaks of PIM-laurate and PID-di-laurate were coeluted in standard reference materials, although the peak areas were different. This means that the standard reference materials used for verifying retention time was not pure, and monoesters and diesters with the same parent moiety may coexist. Therefore, it is speculated that parts I, II and III in Fig. 2B are PS/PI/POE, monoester and diester, respectively. In addition, it can be seen from Fig. 2B that the elution order of the peaks is sorbitol ester > sorbitan ester > isosorbide ester; thus, it is speculated that peaks 1 and 2 are of PS/PI/POE. Peaks 7 and 8 contain PSM-laurate and PIM-laurate. Peaks 11 and 12 contain polysorbate sorbitan dilaurate (PSD-di-laurate) and PID-di-laurate, respectively. The reference standard of polyoxyethylene sorbitan tetralaurate (PSTetra-tetra-laurate) was used to verify our conjecture of the distribution of esters. There are three peaks in the reference standard of tetraester (Fig. 2C). Theoretically, PSTetra-tetra-laurate may contain sorbitan monoester, sorbitan diester, sorbitan triester and sorbitan tetraester. Combined with Fig. 2B, since the first peak of PSTetra-tetra-laurate in Fig. 2C is at peak 11, it belongs to part III. This is an indication that peak 11 may contain PSD-di-laurate and peak 12 may contain PID-di-laurate. It was surmised that parts IV and V in Fig. 2C are triesters and tetraesters of polyoxyethylene sorbitan, respectively. Peaks 14 or 15 might possibly contain polyoxyethylene sorbitan trilaurate (PSTri-tri-laurate). PSTetra-tetra-laurate may be eluted as peaks 17 or 18. Fig. 2D can be used to confirm the positions of the triester and tetraester. Theoretically, polyoxyethylene sorbitol hexaesters will contain esters ranging from sorbitol monoesters to sorbitol hexaesters. In fact, it has three peaks, and the first two peaks are located at position 13 and position 17, respectively, close to the IV and V parts in Fig. 2C. The positions of triesters and tetraesters inferred by Fig. 2D are therefore proven. Fig. 2D shows that there are sorbitol triesters at peak 13 and sorbitol tetraesters near peak 17. This indicates that there is PSTri-tri-laurate after peak 13, and peak 17, or peak 18 may contain PSTetra-tetra-laurate. To sum up, combined with the location results in Figs. 2B–2D, it is preliminarily inferred that peaks 1 and 2 are due to PS/PI/POE, peaks 7 and 8 contain monoesters including PSM-laurate and PIM-laurate, peaks 11–13 may contain diesters like PSD-di-laurate and PID-di-laurate, peaks 14–16 are of PSTri-tri-laurate, and PSTetra-tetra-laurate may be eluted as peak 17 or peak 18. These components were further characterized by UHPLC-Q-TOF-MS.

3.3. Expansion of PCDL

Previous structural polysorbate databases are known to miss some potential variations in structural information derived from the raw materials used in the manufacturing processes, and from the latter themselves [16,37,38]. Here, before mass characterization, the polysorbate database was expanded and the library of possible compositions of PS20 was updated from 1074 compounds to 7765 compounds. With the introduction of this large number of components, the PCDL Manager B.08.00 software was applied to infer the composition of PS20. This was built on the existing PS80 database (Agilent Technologies) for targeted expansion based on the properties of polysorbate substances, by increasing the variety of esters and consideration of fatty acid diversity in PS20. Different combinations between each part of the structure, as well as different arrangements were both considered, as shown in Fig. S3. Specifically, on the basis of stearate, palmitate, laurate and oleate in the existing PS80 database, esters formed by caproic acid, caprylic acid, decanoic acid, myristic acid and linoleic acid were added. According to the structure of PS20, sorbitan can bind with acids to form monoesters, diesters, triesters and tetraesters, while isosorbide and polyoxyethylene can also combine with acids to form monoesters and diesters. Meanwhile, POE, sorbitan and isosorbide may theoretically be considered to combine with 9 kinds of fatty acids to form various esters. In addition, the database contains up to 80° of polymerization for each component (adjusted appropriately according to the composition), while it also considers that a component may be structurally linked to different fatty acids to form mixed fatty acid esters. Therefore, this database contains the mixed diesters, triesters and tetraesters formed by the four most abundant fatty acids (lauric acid, myristic acid, palmitic acid and oleic acid) in PS20. After different arrangements and combinations, the initially established PCDL was expanded to contain 7765 compounds, and the chemical formulas of these compounds were then input into the imported template. The template was then exported to PCDL Manager B.08.00 software to establish the final expanded in-house PCDL for PS20 characterization. After combining the newly established PCDL of PS20 and setting the appropriate parameters in the Qualitative Analysis 10.0 software, the target could be screened for the MS data. The PCDL can be used to search for compounds whose additional ions are H^+, Na^+, and NH_4^+, and whose charge states are $z = 1$ or $z = 2$.

3.4. Structural deduction of PS20 components by MS

To further characterize and confirm the composition of PS20, Q-TOF-MS was employed. According to the PS20 synthesis process, the three parts of its structure were arranged and combined to deduce the components contained in PS20 as much as possible. By searching and comparing the additional ion m/z values measured by UHPLC-Q-TOF-MS with the compounds in PCDL, the components contained in each peak were inferred. The total ion current (TIC) traces of the sample and the standard reference materials obtained by UHPLC-Q-TOF-MS are shown in Figs. S4 and S5. Despite the difference of response intensities, the elution and separation results in the chromatographic system (Fig. 2A) could also be reflected by the TIC trace. The TIC exhibits more overlaps between peaks than those in CAD, and this is possibly caused by the differentiated response of each component. Since components reflected in the peaks of both TIC and CAD chromatograms are not single, and at the same time the MS detector is a more universal and discriminative detector than CAD, differences in peak broadening could be obtained, resulting in greater peak overlapping. The TIC baseline exhibits a more complex composition; the proportion of overlaps between peaks is greater than those in HPLC-CAD, possibly due to the combination of different fatty acids or ions.

To investigate the existence of 11 theoretical components, this study used Qualitative Analysis 10.0 software to extract the mass spectra. On the basis of the aforementioned positioning results, an investigation was conducted; mass spectra were obtained by extracting peaks 1, 2, 7, 8, 12, 13, 15, and 17 from the TIC. The m/z ratio range of the obtained mass spectrum was 100–3000, and the mass spectrum of the target (taking laurate as an example) was searched. The detailed flow chart of the mass spectra of the target component was obtained by extracting peaks 1, 2 and 7 as shown in Fig. 3, and the final mass spectra of peaks 8, 12, 13, 15 and 17 are also shown in the diagram. Finally, 11 theoretical components were found. The mass spectrum exhibits a normal distribution. Taking NH_4^+ as an example, these $[M + NH_4]^+$ masses are 44.0262 Da apart, equivalent to the molecular weight of one ethylene oxide subunit. These $[M+2NH_4]^{2+}$ masses are 22.0131 Da apart.

Combining the extracted mass spectra with the compounds in PCDL, the existence of PS/PI/POE components as peak 1 and peak 2 were verified. The results of component attribution inferred from the MS analysis of PS20 were consistent with the preliminary

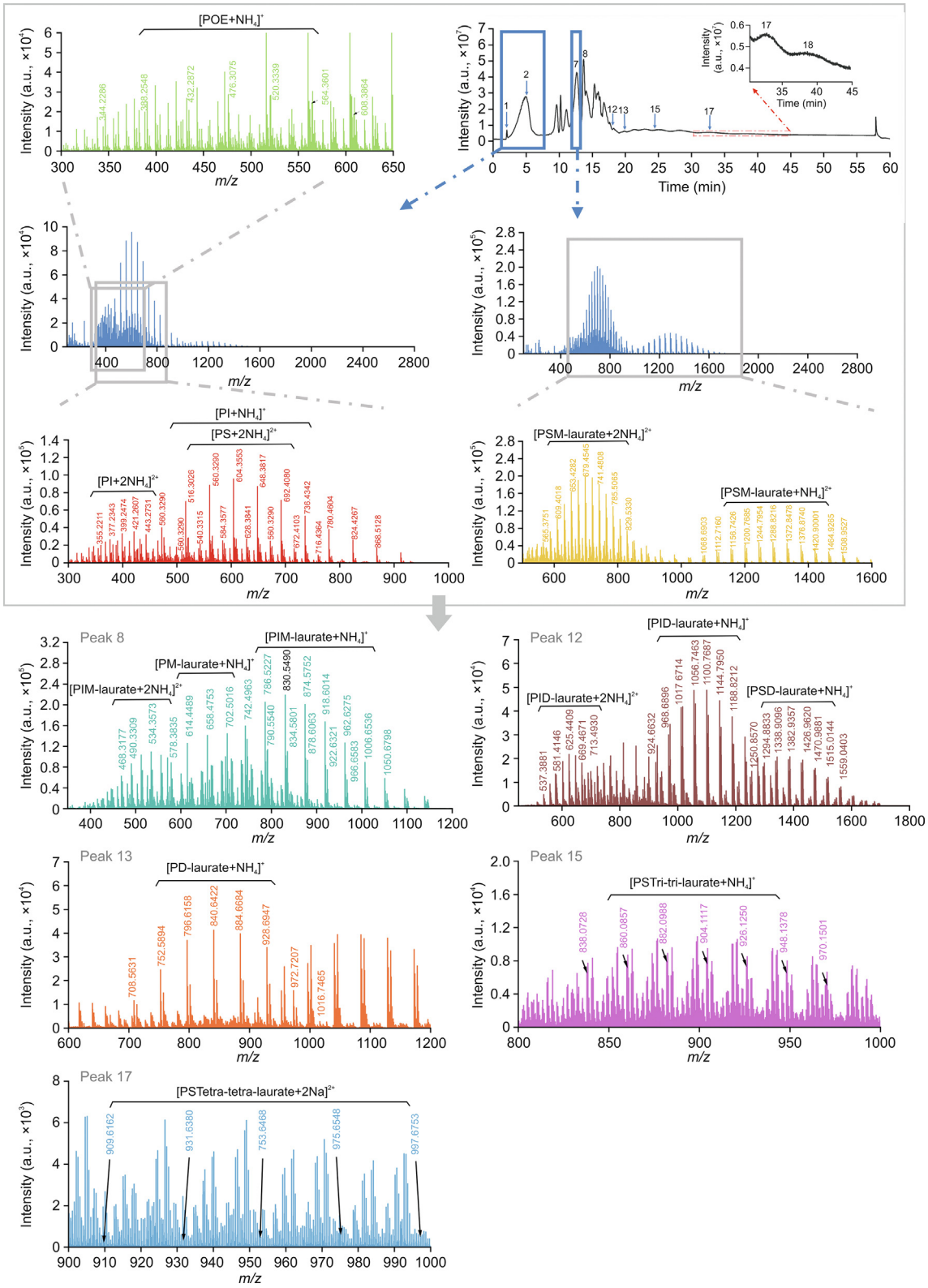

Fig. 3. The flow chart of the mass spectra of the target component is obtained by extracting chromatographic peaks. POE: polyoxyethylene; PI: polyoxyethylene isosorbitan; PS: polyoxyethylene sorbitan; PSM: polyoxyethylene sorbitan monoesters; PIM: polyoxyethylene isosorbitan monoesters; PID:polyoxyethylene isosorbitan diesters; PD: polyoxyethylene diesters; PSTri: polyoxyethylene sorbitan triesters; and PSTetra: polyoxyethylene sorbitan tetraesters.

localization results studied by HPLC-CAD. It also demonstrated the monoester and diester distribution as indicated above. Peaks 7 and 8 contained PSM-laurate and PIM-laurate, respectively. Peak 12 contained PSD-di-laurate, while peak 13 consisted of PID-di-laurate. This is consistent with the previously inferred results that peaks 11–13 may contain PSD-di-laurate and PID-di-laurate. Additionally, combined with the MS results, the analysis recognized PSTri-tri-laurate in peak 15 and PSTetra-tetra-laurate in peak 17 (Note that it had earlier been speculated (see above) that HPLC-CAD analysis inferred the presence of PSTri-tri-laurate in peak 14 or 15). Combined with the MS results, PSTri-tri-laurate and PSTetra-tetra-laurate were eluted as peak 15 and peak 17, respectively. Thus, the main laurate esters in PS20 could be reliably inferred and profiled according to the elution sequence, using MS. Accordingly, it is extended to all components, and compared with the PCDL database to speculate on the identities of the components in the sample. The statistical results on the types of identified components, the range of degree of polymerization of components and the number of compounds obtained after extraction of each peak in 10 batches of samples are listed in Table S1.

Taking sample C1 as an example, the distribution of POE, PS, PI and different esters is shown in Fig. 4. Due to the difference of fatty acids among monoesters, diesters, triesters and tetraesters, the polarity of some components is similar, and the retention time is basically the same. Different esters cannot be completely separated on the reversed-phase column, but the approximate range can be

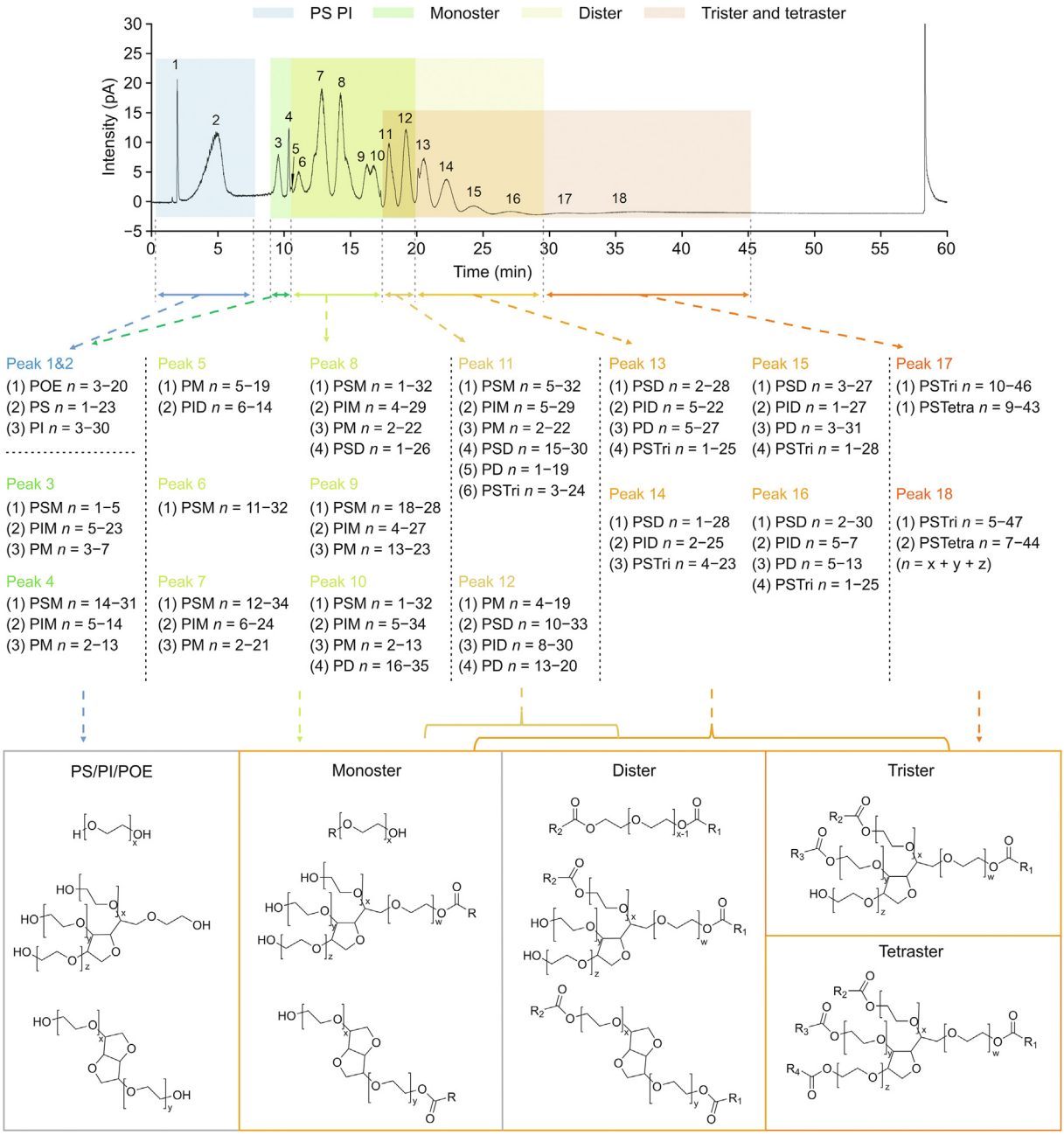

Fig. 4. Distribution of polyoxyethylene (POE), polyoxyethylene sorbitan (PS), polyoxyethylene isosorbitan (PI) and different esters (sample C1). PSM: polyoxyethylene sorbitan monoesters; PIM: polyoxyethylene isosorbitan monoesters; PM: polyoxyethylene monoesters; PID:polyoxyethylene isosorbitan diesters; PSD: polyoxyethylene sorbitan diesters; PD: polyoxyethylene diesters; PSTri: polyoxyethylene sorbitan triesters; and PSTetra: polyoxyethylene sorbitan tetraesters.

determined. It can be observed in this HPLC-CAD method that PS/PI/POE appears in the region of peaks 1–2, and the retention time is about 1.50–7.00 min. The monoester components are eluted in the range of peaks 3–12, and the retention time is about 8.50–18.50 min. The diester component is eluted in the range of peaks 5–16, and the retention time is about 10.20–30.00 min. The triester and tetraester components mainly fall in the range of peaks 11–18, and the retention time is about 16.00–45.00 min. In conclusion, this HPLC-CAD method offered a convenient way of differentiating the components especially the degree of esterification. The information gleaned is critical to further research on the preparation process, and the transportation and storage conditions of PS products.

3.5. Analysis of compounds in PS20 sample by PCDL

According to the grade and validity/expiry period, 10 representative samples were selected from 12 batches of PS20 for study with the following designations: (A–F represent manufacturers; 1–5 represent different batches). The MS results for samples A1, A2, B1, C1, C3, C5, D1, D2, E1 and F1 samples were evaluated and compared. In general, 69–83 components were obtained from these 10 batches of samples, and 1329–1511 compounds were obtained based on different degrees of polymerization. The number of the various components are summarized in Table S2 and Fig. S6. The results (Fig. S6) revealed that the number of esters in the samples were in the following order: diesters > monoesters > triesters > tetraesters. Comparing the number of compounds of PS20 (non-injection) and PS20 (injection) from different manufacturers, it was found that for almost all samples, the number of compounds in monoester and diester classes was comparable. Specifically, the number of compounds in PS20 (injection) from manufacturer C was less than that in their own PS20 (non-injection) product, while the number in PS20 (injection) in the samples from other manufacturers was more than that in PS20 (non-injection). A similar situation was observed for the number of tetraester components in the samples from C and other manufacturers. The results showed that PS20 (injection) from manufacturer C contained fewer triesters and tetraesters. Based on the results, the difference might have originated from the PS20 synthesis processes: PS20 (non-injection) from manufacturer C was synthesized by esterification before etherification, while the converse was true for PS20 (injection). For the former process, sorbitan first undergoes an esterification reaction with coconut oleic acid to obtain the corresponding esterified product. Due to the presence of four hydroxyl groups in sorbitan, there are problems related to the number of esterification sites and the selectivity of esterification sites, resulting in multiple esterification products (there are 15 products theoretically). The efficiency of ethylene oxide insertion of the ester group and hydroxyl groups is different, resulting in poor selectivity of the reaction. As a result, the products affected by this may be more widely distributed. For all batches it can be concluded that the number of triesters and tetraesters can be controlled by the synthesis of the etherification-first process. It can be seen that there is a difference between PS20 (non-injection) and PS20 (injection), and the components of PS20 (injection) are more complex and diverse. Different production processes of the various manufacturers may also lead to differences in the composition of PS20.

3.6. Compositional discrimination of PS20 by HPLC-CAD

Comparison of the HPLC-CAD results shows that the composition of 8 batches of PS20 samples of different grades and of different validity/expiry periods from 6 local (China) and foreign manufacturers were approximately the same, but there were still slight differences (Fig. 5A). The most obvious difference is with respect to peak 5. Samples C3 and F1 had no obvious peak 5. The

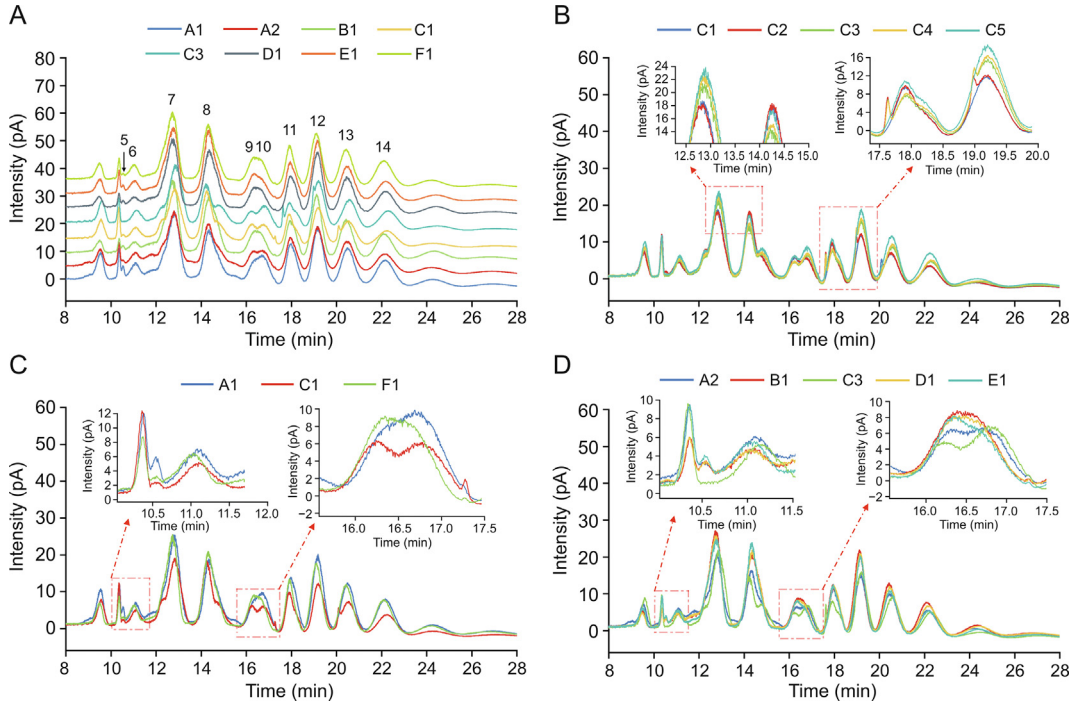

Fig. 5. Comparison of polysorbate 20 (PS20) composition from different sources (sample C1, C3, C4 and C5). (A) Different manufacturers. (B) different grades of PS20 samples from the same manufacturer (manufacturer C). C1, and C2: PS20 (non-injection), C3, C4 and C5: PS20 (injection). (C) PS20 (non-injection) samples from different manufacturers. (D) PS20 (injection) samples from different manufacturers.

bimodal phenomenon of peaks 7 and 8 was obvious in C, and the separation of peaks 9 and 10 was clear for C (C1 and C3). This shows that the components of PS20 products produced by different manufacturers were different. The samples of PS20 (non-injection) and PS20 (injection) from the same manufacturer (C) were compared (Fig. 5B). The chromatogram of C5 (expired sample) is similar to that of C3 and C4 (unexpired sample), indicating that the expiration of the sample stored at room temperature has little effect on the components. The chromatograms of different batches of samples of the same grade (C1 and C2 were for non-injection samples, C3, C4 and C5 for injection) are similar. So were the peak areas. These observations indicate that the contents were basically the same. There is a significant difference between injection samples and non-injection samples. The peak areas of some components of non-injection samples were slightly different from those of samples for injection, notably peaks 7, 8, 11, 12 and 13. The peak areas after peaks 7 and 12 of the samples for injection were higher than those of the non-injection sample, i.e., the contents of the PSM-laurate, diester and polyester components of PS20 (injection) were significantly higher than that of PS20 (non-injection) sample. Additionally, comparing the PS20 (non-injection) samples from different manufacturers (Fig. 5C), the peak 5 of sample A1 was significantly higher than that of the other two samples, and the peak shape of sample C1 was obviously different from that of the other two samples at peaks 7–10. The chromatograms of samples F1 and A1 are comparable, indicating that similar processes for the production of PS20 (non-injection) from the two manufacturers may be applicable. Besides, there are great differences in the samples of PS20 (injection) from different manufacturers (Fig. 5D). Among the samples for injection, B1, D1 and E1 were from foreign manufacturers, and the chromatographic trend was basically the same, which is different from that of A2 and C3 from domestic manufacturers (which can be seen at peaks 7–9). This shows that the composition of the samples for injection was different between foreign manufacturers and domestic manufacturers. Combined with Figs. 5C and 5D, we can see that the composition based on chromatographic analysis of C manufactured domestically was different from that produced by foreign companies, most likely due to varying production processes.

Above all, the chromatographic results show that the sample grade (injection sample or non-injection sample) has the most obvious effect on the components. The contents of non-injection and injection samples from the same factory were different. The relative content of the main component, PSM-laurate, was higher in the injection sample, while diesters and polyesters were also relatively higher. In addition, the components of non-injection samples from domestic and foreign manufacturers may be similar, but the samples for injection are different, that is, the sample origin (domestic or foreign) mainly affect the composition of injection samples. This may mean that the manufacturers exercise control over the synthesis process according to different sample grades (injection and non-injection preparations). It also indicates that domestic and foreign manufacturers have different ways to control the synthesis of injection products.

3.7. HPLC-CAD-based classification analysis

Principal component analysis (PCA) for visualized classification of samples from different origins was conducted to confirm that the minor differences discovered by HPLC-CAD could be differentiated. To reduce the dimensionality of the separated 18 peaks and find the inner combinations of the original specifications, 3 independent variables were refined to explain the relationship, which is the basis for this classification method. Fig. 6 shows that differentiation between samples with different source is possible. The variances were calculated: 46.50% for principal component (PC) 1, 20.60% for

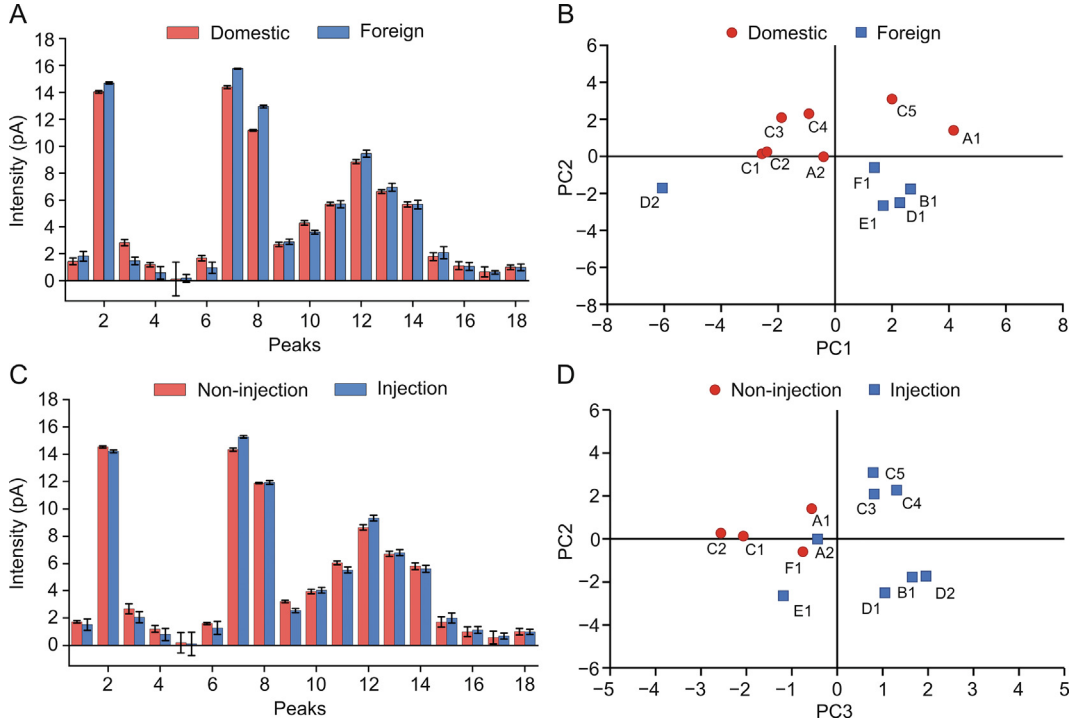

Fig. 6. Classification of samples based on different manufacturing regions and polysorbate 20 (PS20) grades (sample A1, A2, B1, C1, C2, C3, C4, C5, D1, D2, E1, F1). (A) Average relative content obtained by high-performance liquid chromatography with charged aerosol detection (HPLC-CAD) of samples from domestic and foreign manufacturers. (B) Principal component analysis (PCA) plots for the main 18 peaks of PS20 (PC1–PC2). (C) Average relative content obtained by HPLC-CAD of PS20 (non-injection) samples and PS20 (injection) samples. (D) PCA plots for the main 18 peaks of PS20 (PC2-PC3) ($n = 12$).

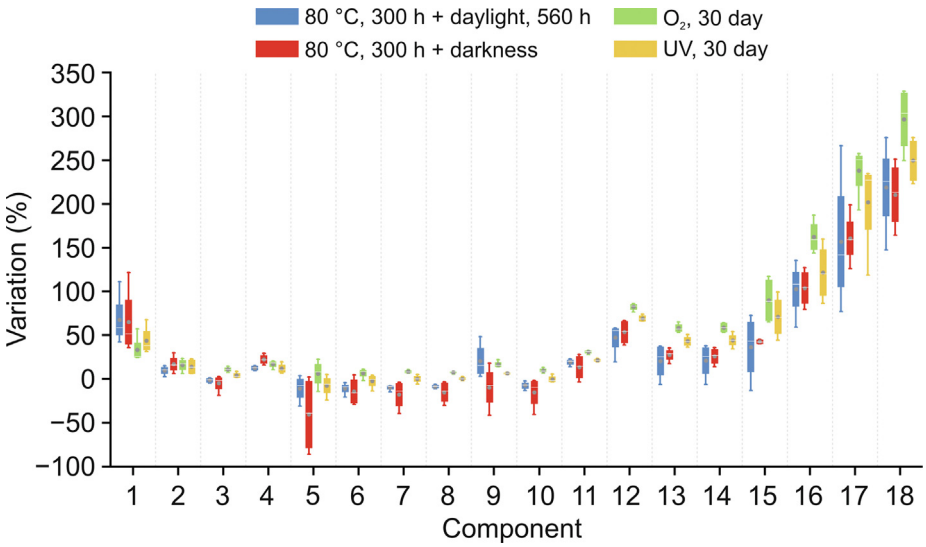

Fig. 7. The variations of the differences in 18 chromatographic peaks before and after degradation under 4 different stress test conditions (n = 16).

PC2, and 12.10% for PC3, totaling 79.20% of explained variance for the first three axes, indicating that the three components provided a relatively good description of the original data. Comparing the average data with respect to 7 domestic and 5 foreign manufacturers, respectively, the analysis showed a consistent composition in these batches with indistinguishable difference (from visual inspection) in relative content (Fig. 6A). However, with the help of PCA tools, PS20 produced in different regions exhibited clear boundaries for division (Fig. 6B). Similarly, Fig. 6D reveals the clustering of PS20 products at different grades (4 batches of PS20 (non-injection) and 8 batches of PS20 (injection)), which could not be discriminated simply by the averaged statistics in Fig. 6C. Although there were also differences between different production batches from the same manufacturer, the results prove that PS20 of different sources can be clearly separated as shown in the PCA using the peak areas of 18 peaks acquired from HPLC-CAD as chemotaxonomic markers.

3.8. Components investigation under forced degradation

To determine whether the degradation had an effect on PS20, the components were studied based on stress tests. Four degradation conditions (oxygen atmosphere (air in containers of PS20 was replaced by filling with oxygen), ultraviolet (UV) irradiation, 80 °C under darkness, and 80 °C under sunlight) were applied, and four batches of samples (A1, B1, C1, and C3) were selected for analysis. Experimental details of the stress tests are shown in the Supplementary data. Also, under these four conditions for 30 days, the components were analyzed by the aforementioned HPLC-CAD method after 10 days and 30 days, respectively. The chromatograms of samples at 10 days and 30 days under different conditions (Figs. S7 and S8), and the chromatographic comparison under the same conditions (Fig. S9) were obtained. In order to make the analysis more valid and accurate, the difference of the ratio of peak area to sample concentration of 18 chromatographic peaks before and after degradation was calculated. The results showed that, on the whole, the components in peaks 1 to 4 increased, those in peaks 5 to 10 decreased, and those in peaks 11 to 18 increased. According to MS results, the changing three segments can be divided into PS/PI/POE and monoester, diester, triester and tetraester. It is known from a previous study that polyesters are sensitive to oxidation induced by 2,2′-azobis (2-amidinopropane) dihydrochloride, and they are preferentially degraded first before the monoesters [17]. The first increase of triester and tetraester may be due to the fact that the oxidation was not strong enough in the absence of a free radical initiator. In the stress tests, when the degraded diesters led to increase of monoesters in the early stage of the reaction, the resulting free fatty acids may combine with each component, resulting in the increase of triester and tetraester content. Combined with the results of the stress tests at 10-day mark, it was found that during the entire test, the components of PS/PI/POE and monoester decreased at first and then increased. The components of diester decreased at first and then went up, while the converse was true for the triester and tetraester components. This shows that with the progress of the experiment, triesters and tetraesters began to degrade and form diesters or monoesters (thus increasing the content of the latter two).

In addition, the variations of the differences before and after degradation (the ratio of the difference to the initial value) were calculated (Fig. 7). The results showed that heating has a significant impact on component changes, whether under light or dark conditions, as the differences of both red and blue data points are significant. Comparing the four conditions, it was also found that the components of each part increased in the oxygenated state. Under oxygen, the reaction was relatively intense, and there was increase in diester content due to hydrolysis of polyesters. Thus, the overall difference of major components of the contents was positive. The detailed variations of each component under these four degradation conditions are listed in Table S3. We can also conclude that the influences on components of samples from different sources may be different depending upon various conditions. Moreover, different from the other two non-injection samples (A1 and C1), the diester components of B1 and C3 (injection) under UV conditions were higher. This indicated that PS20 (injection) underwent greater degradation by UV, suggesting that it should be stored away from light.

4. Conclusions

Here, we proposed a rapid and simple HPLC-CAD method for discriminating PS20 of different qualities/grade based on different processes or from different manufacturers, both local (China) and foreign. We successfully achieved separation of 18 peaks and fulfilled characterization of the composition distribution. With precise

quantitative results of the main components, PS20 samples from different origins could be effectively differentiated. It was also found that different synthesis pathways have a significant impact on the number and distribution of compounds observed. Additionally, long-term degradation experiments using four different forced degradation conditions were considered. Among all the batches of samples, it was observed that the components in peaks 2–4 remained relatively stable throughout the process, while certain esters were affected, particularly by heating and UV. In conclusion, a simple and feasible quantitative and characterization method for PS20 composition was established. By this means, a comprehensive polysorbate compound database and library to facilitate quick matching and searching of similar components was established. Such an independent database, integrated with analysis strategies, can provide a practical and reliable approach not only for process control and quality assurance but also for further research and development or process optimization in the production of polysorbate products.

CRediT author statement

Shi-Qi Wang: Investigation, Validation, Methodology, Data curation, Writing - Original draft preparation; **Xun Zhao**: Investigation; **Li-Jun Zhang**, and **Yue-Mei Zhao**: Data curation; **Lei Chen**: Supervision; **Jin-Lin Zhang**: Data curation; **Bao-Cheng Wang**, **Sheng Tang, Tom Yuan, and Yaozuo Yuan**: Writing - Reviewing and Editing; **Mei Zhang**: Supervision; **Hian Kee Lee**: Writing - Reviewing and Editing, Supervision; **Hai-Wei Shi**: Conceptualization, Reviewing and Editing, Supervision.

Declaration of competing interest

The authors declare that there are no conflicts of interest.

Acknowledgments

The authors are grateful for the financial support from the Science Research Program Project for Drug Regulation, Jiangsu Drug Administration, China (Grant No.: 202207), the National Drug Standards Revision Project, China (Grant No.: 2023Y41), the National Natural Science Foundation of China, China (Grant No.: 22276080), and the Foreign Expert Project, China (Grant No.: G2022014096L).

Appendix A. Supplementary data

Supplementary data to this article can be found online at https://doi.org/10.1016/j.jpha.2023.12.019.

References

[1] R. Muzzalupo, L. Tavano, C.O. Rossi, et al., Synthesis and properties of methacrylic-functionalized tween monomer networks, Langmuir 25 (2009) 1800–1806.
[2] A. Raval, P. Bahadur, A. Raval, Effect of nonionic surfactants in release media on accelerated *in-vitro* release profile of sirolimus eluting stents with biodegradable polymeric coating, J. Pharm. Anal. 8 (2018) 45–54.
[3] H. Kumari, S.R. Kline, J.L. Atwood, Aqueous solubilization of hydrophobic supramolecular metal-organic nanocapsules, Chem. Sci. 5 (2014) 2554–2559.
[4] C. Caddeo, M.L. Manca, J.E. Peris, et al., Tocopherol-loaded transfersomes: *in vitro* antioxidant activity and efficacy in skin regeneration, Int. J. Pharm. 551 (2018) 34–41.
[5] C. Yucel, V. Quagliariello, R.V. Iaffaioli, et al., Submicron complex lipid carriers for curcumin delivery to intestinal epithelial cells: Effect of different emulsifiers on bioaccessibility and cell uptake, Int. J. Pharm. 494 (2015) 357–369.
[6] R. Jain, R.K. Yadav, Voltammetric behavior of sedative drug midazolam at glassy carbon electrode in solubilized systems, J. Pharm. Anal. 2 (2012) 123–129.
[7] A. Kannan, I.C. Shieh, P.G. Negulescu, et al., Adsorption and aggregation of monoclonal antibodies at silicone oil-water interfaces, Mol. Pharmaceutics 18 (2021) 1656–1665.
[8] A.S. Roy, A.K. Dinda, N.K. Pandey, et al., Effects of urea, metal ions and surfactants on the binding of baicalein with bovine serum albumin, J. Pharm. Anal. 6 (2016) 256–267.
[9] A.D. Kanthe, M. Krause, S. Zheng, et al., Armoring the interface with surfactants to prevent the adsorption of monoclonal antibodies, ACS Appl. Mater. Interfaces 12 (2020) 9977–9988.
[10] T.A. Khan, H.C. Mahler, R.S.K. Kishore, Key interactions of surfactants in therapeutic protein formulations: A review, Eur. J. Pharm. Biopharm. 97 (2015) 60–67.
[11] J.S. Katz, Y. Tan, K. Kuppannan, et al., Amino-acid-incorporating nonionic surfactants for stabilization of protein pharmaceuticals, ACS Biomater. Sci. Eng. 2 (2016) 1093–1096.
[12] K. Yang, A. Hewarathna, I. Geerlof-Vidavsky, et al., Screening of polysorbate-80 composition by high resolution mass spectrometry with rapid H/D exchange, Anal. Chem. 91 (2019) 14649–14656.
[13] J.R. Snelling, C.A. Scarff, J.H. Scrivens, Characterization of complex polysorbate formulations by means of shape-selective mass spectrometry, Anal. Chem. 84 (2012) 6521–6529.
[14] Y. Li, D. Hewitt, Y.K. Lentz, et al., Characterization and stability study of polysorbate 20 in therapeutic monoclonal antibody formulation by multidimensional ultrahigh-performance liquid chromatography-charged aerosol detection-mass spectrometry, Anal. Chem. 86 (2014) 5150–5157.
[15] N. Doshi, B. Demeule, S. Yadav, Understanding particle formation: Solubility of free fatty acids as polysorbate 20 degradation byproducts in therapeutic monoclonal antibody formulations, Mol. Pharm. 12 (2015) 3792–3804.
[16] D.H. Evers, T. Schultz-Fademrecht, P. Garidel, et al., Development and validation of a selective marker-based quantification of polysorbate 20 in biopharmaceutical formulations using UPLC QDa detection, J. Chromatogr. B Anal. Technol. Biomed. Life Sci. 1157 (2020), 122287.
[17] S. Dubey, R. Giovannini, Stability of biologics and the quest for polysorbate alternatives, Trends Biotechnol 39 (2021) 546–549.
[18] X. Li, Z. Wang, B. Zheng, et al., Novel strategy to rapidly profile and identify oxidized species of polysorbate 80 using ultra-high-performance liquid chromatography coupled with high-resolution mass spectrometry, Anal. Chem. 95 (2023) 9156–9163.
[19] K. Zhang, J.D. Pellett, A.S. Narang, et al., Reactive impurities in large and small molecule pharmaceutical excipients - A review, Trac Trends Anal. Chem. 101 (2018) 34–42.
[20] A. Tomlinson, B. Demeule, B. Lin, et al., Polysorbate 20 degradation in biopharmaceutical formulations: Quantification of free fatty acids, characterization of particulates, and insights into the degradation mechanism, Mol. Pharmaceutics 12 (2015) 3805–3815.
[21] N. Doshi, J. Martin, A. Tomlinson, Improving prediction of free fatty acid particle formation in biopharmaceutical drug products: Incorporating ester distribution during polysorbate 20 degradation, Mol. Pharm. 17 (2020) 4354–4363.
[22] M. Dwivedi, M. Blech, I. Presser, et al., Polysorbate degradation in biotherapeutic formulations: Identification and discussion of current root causes, Int. J. Pharm. 552 (2018) 422–436.
[23] M. Manaargadoo-Catin, A. Ali-Cherif, J.L. Pougnas, et al., Hemolysis by surfactants: A review, Adv. Colloid Interface Sci. 228 (2016) 1–16.
[24] J. Ye, L. Li, J. Yin, et al., Tumor-targeting intravenous lipid emulsion of paclitaxel: Characteristics, stability, toxicity, and toxicokinetics, J. Pharm. Anal. 12 (2022) 901–912.
[25] S. Yang, J. Liu, Y. Chen, et al., Reversal effect of Tween-20 on multidrug resistance in tumor cells *in vitro*, Biomed. Pharmacother. 66 (2012) 187–194.
[26] D. Hewitt, M. Alvarez, K. Robinson, et al., Mixed-mode and reversed-phase liquid chromatography-tandem mass spectrometry methodologies to study composition and base hydrolysis of polysorbate 20 and 80, J. Chromatogr. A 1218 (2011) 2138–2145.
[27] Q. Zhang, Y. Meng, H. Yang, et al., Quantitative analysis of polysorbates 20 and 40 by matrix-assisted laser desorption/ionization time-of-flight mass spectrometry, Rapid Commun. Mass Spectrom. 27 (2013) 2777–2782.
[28] N. Glücklich, S. Carle, J. Buske, et al., Assessing the polysorbate degradation fingerprints and kinetics of lipases - how the activity of polysorbate degrading hydrolases is influenced by the assay and assay conditions, Eur. J. Pharm. Sci. 166 (2021), 105980.
[29] M. Dwivedi, J. Buske, F. Haemmerling, et al., Acidic and alkaline hydrolysis of polysorbates under aqueous conditions: Towards understanding polysorbate degradation in biopharmaceutical formulations, Eur. J. Pharm. Sci. 144 (2020), 105211.
[30] J. Kim, J. Qiu, Quantitation of low concentrations of polysorbates in high protein concentration formulations by solid phase extraction and cobalt-thiocyanate derivatization, Anal. Chim. Acta 806 (2014) 144–151.
[31] A. Martos, M. Berger, W. Kranz, et al., Novel high-throughput assay for polysorbate quantification in biopharmaceutical products by using the fluorescent dye DiI, J. Pharm. Sci. 109 (2020) 646–655.
[32] D. Hewitt, T. Zhang, Y.H. Kao, Quantitation of polysorbate 20 in protein solutions using mixed-mode chromatography and evaporative light scattering detection, J. Chromatogr. A 1215 (2008) 156–160.

[33] T. Diederichs, J.J. Mittag, J. Humphrey, et al., Existence of a superior polysorbate fraction in respect to protein stabilization and particle formation? Int. J. Pharm. 635 (2023), 122660.
[34] S. Fekete, K. Ganzler, J. Fekete, Simultaneous determination of polysorbate 20 and unbound polyethylene-glycol in protein solutions using new core-shell reversed phase column and condensation nucleation light scattering detection, J. Chromatogr. A 1217 (2010) 6258–6266.
[35] S. Lippold, S.H.S. Koshari, R. Kopf, et al., Impact of mono- and poly-ester fractions on polysorbate quantitation using mixed-mode HPLC-CAD/ELSD and the fluorescence micelle assay, J. Pharm. Biomed. Anal. 132 (2017) 24–34.
[36] X. Zhou, X. Meng, L. Cheng, et al., Development and application of an MS^{ALL}-based approach for the quantitative analysis of linear polyethylene glycols in rat plasma by liquid chromatography triple-quadrupole/time-of-flight mass spectrometry, Anal. Chem. 89 (2017) 5193–5200.
[37] Z. Wang, Y. Wang, C. Tie, et al., A fast strategy for profiling and identifying pharmaceutic excipient polysorbates by ultra-high performance liquid chromatography coupled with high-resolution mass spectrometry, J. Chromatogr. A 1609 (2020), 460450.
[38] O.V. Borisov, J.A. Ji, Y.J. Wang, et al., Toward understanding molecular heterogeneity of polysorbates by application of liquid chromatography-mass spectrometry with computer-aided data analysis, Anal. Chem. 83 (2011) 3934–3942.
[39] T. Vehovec, A. Obreza, Review of operating principle and applications of the charged aerosol detector, J. Chromatogr. A 1217 (2010) 1549–1556.
[40] Q. Xu, S. Tan, Quantitative analysis of 3-isopropylamino-1, 2-propanediol as a degradation product of metoprolol in pharmaceutical dosage forms by HILIC-CAD, J. Pharm. Anal. 9 (2019) 431–436.